Journal of Alloys and Compounds 510 (2012) 141–146

Contents lists available at SciVerse ScienceDirect

Journal of Alloys and Compounds

journal homepage: www.elsevier.com/locate/jallcom

Effect of Fe substitution on magnetic properties of antiferromagnetic Heusler alloy Ru_2MnGe

S. Mizusaki[a,*], A. Douzono[a], T. Ohnishi[a], T.C. Ozawa[b], H. Samata[c], Y. Noro[d], Y. Nagata[a]

[a] Department of Electronics and Electrical Engineering, College of Science and Engineering, Aoyama Gakuin University, Sagamihara, Kanagawa 229-8558, Japan
[b] International Center for Materials Nanoarchitectonics, National Institute for Materials Science, Tsukuba, Ibaraki 305-0044, Japan
[c] Graduate School of Maritime Sciences, Kobe University, Higashinada, Kobe, Hyogo 658-0022, Japan
[d] Kawazoe Frontier Technologies, Co. Ltd. Kuden, Sakae, Yokohama, Kanagawa 931-113, Japan

ARTICLE INFO

Article history:
Received 27 July 2010
Received in revised form 21 August 2011
Accepted 4 September 2011
Available online 10 September 2011

PACS:
72.15.Gd
72.15.−v
72.25.Ba
75.30.Gw
75.47.−m
75.47.Np

Keywords:
Metals and alloys
Magnetoresistance
Magnetic measurement

ABSTRACT

The present study reveals that the correlation between the magnetic properties with composition x in the polycrystalline $Ru_2Mn_{1-x}Fe_xGe$ system. Hard ferromagnetic properties appeared at the intermediate composition between antiferromagnetic Ru_2MnGe with soft ferromagnetic Ru_2FeGe. $Ru_2Mn_{0.6}Fe_{0.4}Ge$ shows an anisotropic and negative magnetoresistance (MR) effect more than 8% although the both end materials are small MR effect less than 1%. These experimental results correlate the variation in MR ratio with that of coercive field as a function of x. Moreover, the correlation is shown at the boundary of magnetism between antiferromagnetic and ferromagnetic. Therefore, the present experimental results imply that the coexistence of antiferromagnetic and soft ferromagnetic leads to induce the MR effect in this system.

1. Introduction

Heusler alloy systems have attracted renewed attention because the half-metallic ferromagnetic Heusler alloy [1–3] can be used as a spin-filter material for TMR devices on the field of the development of tunnel magnetoresistance (TMR) device. Therefore, it is very important to found novel half metallic materials for the further development of spintronic devices. For example, a magnetic tunneling junction (MTJ) with a thin film electrode of full Heusler alloy $Co_2Cr_{0.6}Fe_{0.4}Al$ shows large TMR at room temperature [4–5]. For $Co_2Cr_{0.6}Fe_{0.4}Al$ [6], it was reported to show a large magnetoresistive effect under a small magnetic field at room temperature [6–10]. The experimental and theoretical studies on the electronic structure of the $Co_2Cr_{1-x}Fe_xAl$ system [11,12] revealed that the full Heusler alloy $Co_2Cr_{0.6}Fe_{0.4}Al$ is a half metallic ferromagnet with high Curie temperature.

Many studies have been performed for the 3*d*-, 4*d*- or 5*d*-transition metal based systems to discover new functional full Heusler alloy systems. It is generally believed that the electron–electron Coulomb repulsion strength U among the d electrons decreases when base element changes from 3*d* to 4*d*/5*d* elements due to the difference in the spatial expanse of d-orbitals. Moreover, the difference between the 3*d* and 4*d*/5*d* electrons seems to affect on the interplay between the chemical composition and electron correlation. Therefore, drastic changes in the magnetic and transport properties are expected for 4*d*- or 5*d*-transition metal based Heusler alloys in comparison with the 3*d*-transition metal based alloys.

Among the 4*d*- or 5*d*-transition metal based Heusler alloys it was reported that Ru_2FeZ (Z = Ge, Sn) [13,14] shows ferromagnetism, while Ru_2FeSi [15–17] and Ru_2MnZ (Z = Sn, Si, Sb, Ge) [13] are antiferromagnetic. Moreover, the existence of a polarized conduction electron band has been reported for Ru_2FeGe [14]. Therefore, it is interesting to study the influence of the crossover from antiferromagnetism to ferromagnetism on the transport properties in the $Ru_2Mn_{1-x}Fe_xGe$ system. In this paper, we synthesized the Ru based Heusler alloy system $Ru_2Mn_{1-x}Fe_xGe$, and investigated the

* Corresponding author.
E-mail address: smizusaki@ee.aoyama.ac.jp (S. Mizusaki).

0925-8388/$ – see front matter © 2011 Published by Elsevier B.V.
doi:10.1016/j.jallcom.2011.09.017

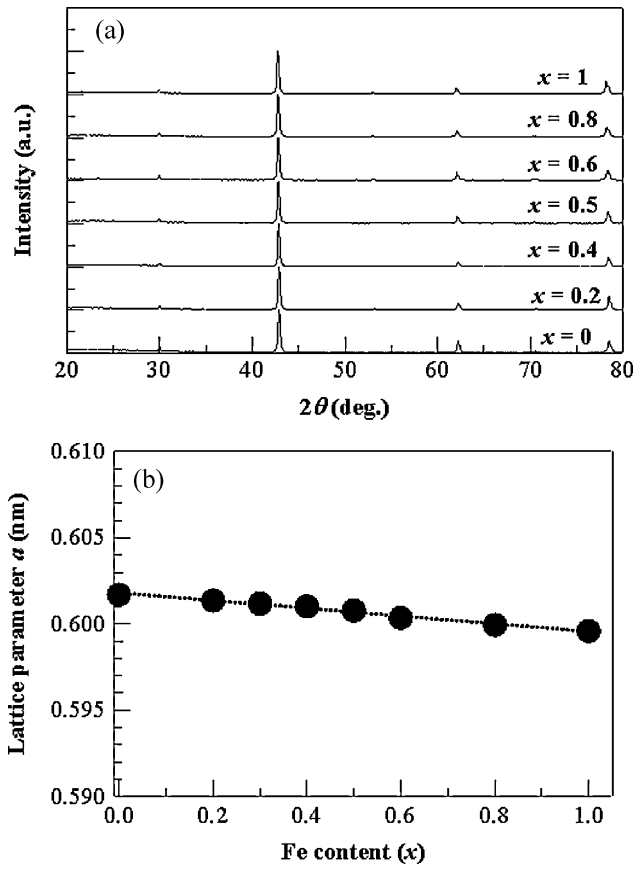

Fig. 1. (a) Powder XRD profiles of $Ru_2Mn_{1-x}Fe_xGe$ and (b) refined cubic lattice parameter a of $Ru_2Mn_{1-x}Fe_xGe$ as a function of Fe content x.

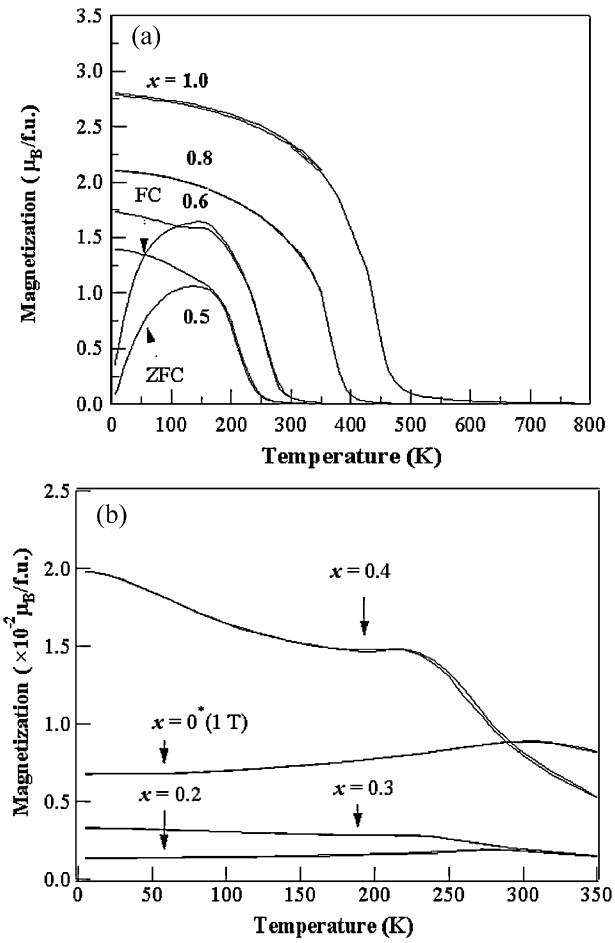

Fig. 2. (a) Temperature dependence of the magnetization of $Ru_2Mn_{1-x}Fe_xGe$ for $x < 0.5$ and (b) that for $x \geq 0.5$.

crystallography, magnetism, and transport properties to be discuss the interplay between magnetism and transport properties.

2. Experiment

Polycrystalline $Ru_2Mn_{1-x}Fe_xGe$ samples were prepared by arc melting. Stoichiometric amounts of the elemental constituents were melted in a zirconium-gettered Ar atmosphere. The polycrystalline ingots were sealed into an evacuated quartz ampoule. The ampoule was heated to 1173 K and after being kept for 72 h, the ampoule was quenched into water. The crystallographic properties were characterized by the X-ray powder diffraction using Cu-Kα radiation. Lattice constants were obtained by the Rietveld method. The magnetic properties were characterized by SQUID magnetometer and VSM. Resistivity measurements were performed by the standard four-probe method under an applied field up to 5 T. The magnetoresistance ratio (MR ratio) is defined as $\Delta\rho^{MR}/\rho = [\rho(B)-\rho(0)]/\rho(0)$.

3. Results and discussion

3.1. Structural properties

The XRD profiles for $Ru_2Mn_{1-x}Fe_xGe$ samples in Fig. 1(a) show that all samples are single phase with $Fm3m$ symmetry structure at room temperature. All samples shows the superlattice reflection from the (1 1 0) plane; however, no reflection of the (1 1 1) plane is shown. The analysis of present XRD profiles indicates that the polycrystalline $Ru_2Mn_{1-x}Fe_xGe$ have the B_2-type ordering states. Lattice parameters were obtained by assuming the space group $Fm3m$ (No. 225) [14] with the S ($=R_{wp}/R_e$) value for all samples to be less than 1.3. The refinement for Ru_2FeGe shows that Fe and Ge atoms are ordered on each crystallographic position with a disorder level of approximately 2%. That for $Ru_2Mn_{0.5}V_{0.5}Ge$ indicates that Mn/Fe atoms mainly are same crystallographic position and that they are partially exchanged to Ge atoms with a disorder level of approximately 5%. The lattice parameter a for Fe-content dependence as shown in Fig. 1(b) decreases monotonically from 0.602 nm for Ru_2MnGe to 0.600 nm for Ru_2FeGe with the 0.284×10^{-4} nm for the error of lattice constants. These results additionally indicate that Fe atom has been substituted mainly to Mn atom.

A recent synchrotron-based XRD study for $Co_2Mn_{1-x}Ti_xSn$ system by Graf et al. [18] suggests that even if the lattice constant change monotonically as function of its content, a phase separation may take place and then, the atom are not uniformly distributed on the crystallographic positions, however, our experimental result shows no peak separation at the (2 2 0) refraction. Then, there is no phase separation on the $Ru_2Mn_{1-x}Fe_xGe$ system.

3.2. Magnetic properties

Temperature dependence of the magnetization for $Ru_2Mn_{1-x}Fe_xGe$ is shown in Fig. 2(a) for the sample of $x = 0$–0.4 and in Fig. 2(b) for that of $x = 0.5$–1, respectively. The samples of $x = 0$, 0.2, and 0.3 show the typical antiferromagnetic temperature dependence, whereas the samples of $x = 0.5$–1 show ferromagnetic behavior. In particular, the Fe rich samples ($x = 0.8$ and 1) show a typical ferromagnetic order. The samples of $x = 0.5$ and 0.6 show a large thermal hysteresis between the zero-field cooled and the field cooled curves. The sample of $x = 0.4$ shows a both antiferromagnetic and ferromagnetic contribution. The temperature dependence of the magnetization indicates that the samples with $x = 0.4$–0.6 has a both antiferromagnetic and ferromagnetic contributions.

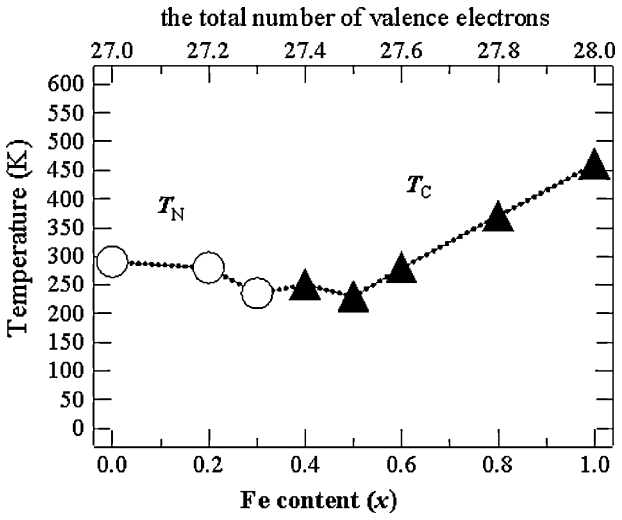

Fig. 3. Magnetic transition temperatures of $Ru_2Mn_{1-x}Fe_xGe$ as a function of Fe content x.

Fig. 3 summarizes the magnetic transition temperature (Néel temperature T_N or Curie temperature T_C) of the $Ru_2Mn_{1-x}Fe_xGe$ system as a function of Fe content x. All samples have transition temperatures more than 200 K. T_N decreases from the value of 300 K for $x = 0$ (Ru_2MnGe) [19] to 230 K for $x = 0.3$ via 280 K for $x = 0.2$. This means that Fe doping suppress the antiferromagnetic contribution. After the magnetism of the system changes from antiferromagnetism to ferromagnetism at around $x = 0.4$, Curie temperature T_C displace T_N and increase linearly with the Fe content after $x = 0.5$. This result indicates that Fe doping induce the ferromagnetism.

Magnetic-field dependence of the magnetization at 5 K for $Ru_2Mn_{1-x}Fe_xGe$ as shown in Fig. 4(a) shows that the magnetic properties for $Ru_2Mn_{1-x}Fe_xGe$ change from the antiferromagnetic to soft ferromagnetic with increase of the amount of Fe content. The samples of $x = 0$–0.3 show a linear field dependence as displayed in the inset of Fig. 4(a). However, there is no consistent trend with the Fe content as shown in inset of Fig. 4(a). The one of the possibility is that the sample of $x = 0.35$ would be an initial magnetization states as ferromagnetic material with large coercivity, hence, the ferromagnetic states could not be observed by the weak applied magnetic fields with the present experiment. The sample of $x = 0.45$ shows the hysteresis loops with a large coercivity of 0.41 T and the saturation magnetization of 0.8 μ_B/f.u. In addition, it is noted that the center of the hysteresis loop of $x = 0.45$ shifts slightly to the direction of negative field and positive magnetization, which is a typical feature of the mictomagnetism. On the other hand, the sample of $x = 1$ has a large saturation magnetization (3.1 μ_B/f.u.) with a small coercivity.

The saturation magnetization and the coercivity have been summarized in Fig. 4(b) as a function of Fe-content x. The saturation magnetization is 3.1 and 1.5 μ_B/f.u. for Ru_2FeGe and $Ru_2Mn_{0.5}Fe_{0.5}Ge$, respectively. Magnetization appears at around $x = 0.4$ and linearly increases from $x = 0.6$ as increase of the Fe content. On the other hand, coercivity appears at about $x = 0.4$ and it decreases after having a maximum (4.13 kOe = 0.41 T) at $x = 0.45$. This means that the characteristic of the ferromagnetism changes from hard magnetic property ($Ru_2Mn_{0.6}Fe_{0.4}Ge$) to soft magnetic one (Ru_2FeGe) as the Fe content increases.

From the results in Figs. 3 and 4, the magnetism of the $Ru_2Mn_{1-x}Fe_xGe$ system can be classified into three groups depending on their characteristics. They are antiferromagnetic group-I ($0 \le x < 0.4$), ferromagnetic group-II ($0.4 \le x \le 0.6$) with large coercivity, and ferromagnetic group-III ($0.8 \le x \le 1$) with small coercivity.

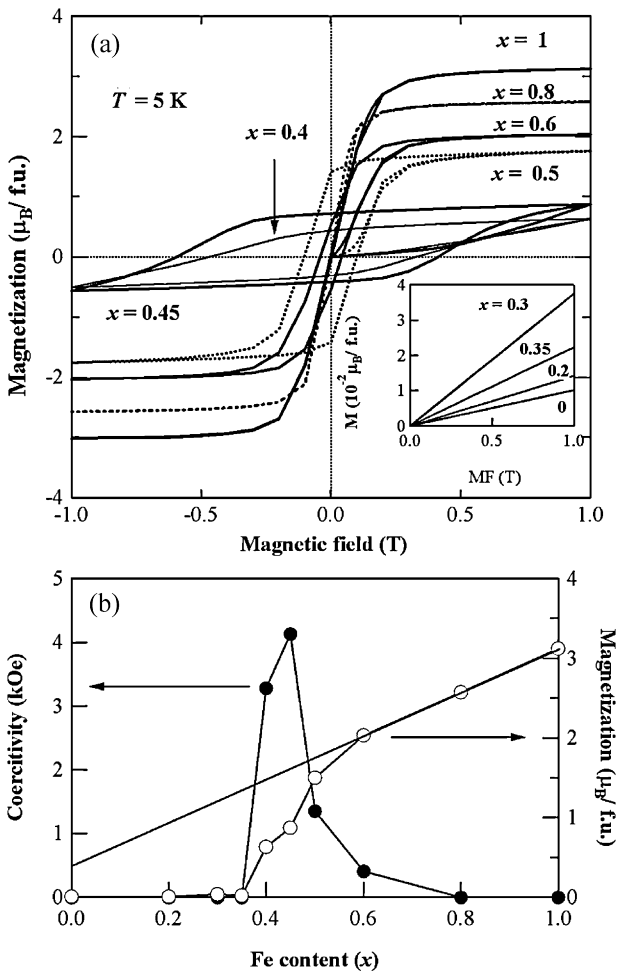

Fig. 4. (a) Isothermal magnetization curve $M(H)$ for $Ru_2Mn_{1-x}Fe_xGe$ at 5 K. The inset of the figure shows those of the samples with $x = 0$ and 0.3. (b) Saturation magnetization (filled circle) and coercivity (open circle) as a function of Fe content x.

In ferromagnetic group-III, the magnetization of 3.1 μ_B/f.u. for Ru_2FeGe is attributed to Fe atom assuming a non-magnetic state of Ru atom. The experimental values of the magnetization (total magnetic moment) are compared with the values calculated by the Slater-Pauling rule (SP-rule) because it is well known that the SP-rule well describes the total magnetic moment of 3d-baesd compounds [20]. The SP-rule represents the total moment as $M_t = Z_t - 24$, where M_t is the total moment in μ_B per formula unit and Z_t is the total number of valence electrons. The M_t of Ru_2FeGe ($Z_t = 28$) and Ru_2MnGe ($Z_t = 27$) are 4 and 3 μ_B/f.u., respectively. These values disagree with the experimental values. Similar discrepancy is observed for other ferromagnetic materials such as Cu_2MnAl, Pd_2MnSn, and Pd_2MnSb [13,20]. The discrepancy observed for antiferromagnetic Ru_2MnGe was pointed out already [13]. However, the present discrepancy for Ru_2FeGe would be caused by the atomic disorder on crystallographic positions between Fe and Ge, which strongly dominates the saturation magnetization.

In ferromagnetic group-II, Fig. 4(b) for the appearance of coercivity indicate that there is a ferromagnetic anisotropy in the middle range of $Ru_2Mn_{1-x}Fe_xGe$ system, and that it would be originated by the coexistence between the antiferromagnetic and the ferromagnetic interaction. Fig. 5 summarized the magnetic properties for the sample of $x = 0.45$. Large thermal hysteresis was observed between the ZFC and the FC condition and their magnetic hysteresis shows different magnetic field dependence. This result

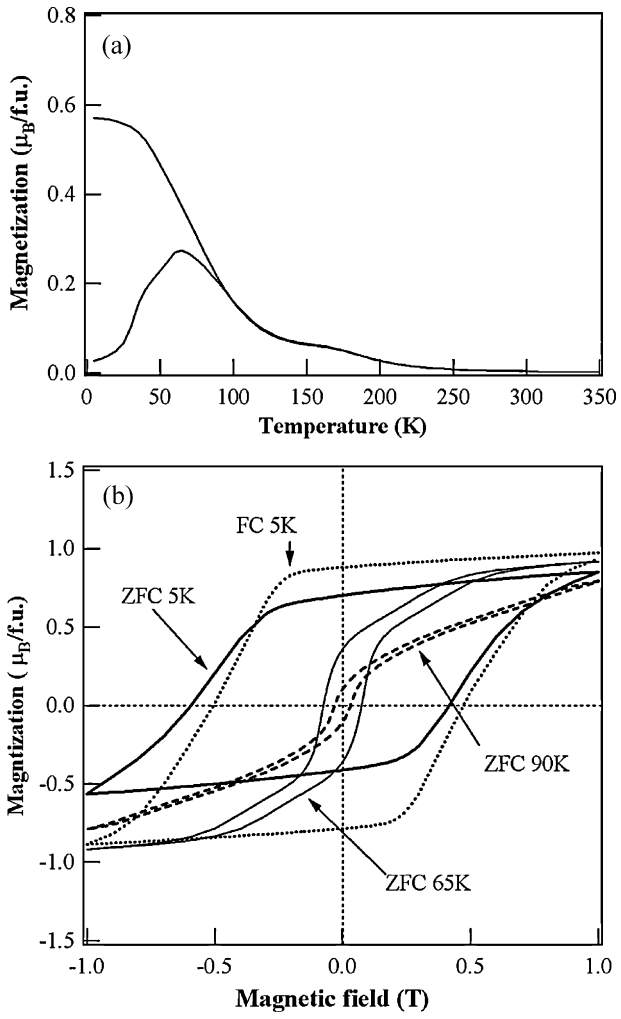

Fig. 5. (a) Temperature dependence of the magnetization of $Ru_2Mn_{0.65}Fe_{0.45}Ge$ under 0.1 T and (b) isothermal magnetization curve $M(H)$ for $Ru_2Mn_{0.65}Fe_{0.45}Ge$ at 5 K, 65 K and 90 K under ZFC and that at 5 K under FC.

indicates the magnetization process is difference between the ZFC and the FC condition. The discrepancy of the magnetization process would be caused by the difference on the magnetic anisotropy between both cooling conditions.

These results indicate that these magnetic behaviors in the ferromagnetic group-II ($0.4 \leq x \leq 0.6$) would be induced by the coexistence of the both antiferromagnetic and ferromagnetic contributions. The magnetic anisotropy and a large coercivity would be originated by the pinned ferromagnetic Fe moment induced by this magnetic coexistence states. The origin of magnetic anisotropy can be inferred by the following. Fe moment behaves a soft ferromagnetic as shown in the magnetization process of Ru_2FeGe shown in Fig. 4, and Mn moment in Ru_2MnGe has an antiferromagnetic magnetic anisotropy in the [1 1 1] direction [19]. Antiferromagnetic Mn moments aligned along the [1 1 1] direction could pin nearest neighbor ferromagnetic Fe moments via magnetic exchange interaction.

The coexistence of the both antiferromagnetic and ferromagnetic contributions can be explained by the macroscopic phase separation material such as $Co_2Mn_{1-x}Ti_xSn$ system[18] or to that of the typical mictomagnetism [21]. In case of the macroscopic phase separation, these observations might be explained by the macroscopic phase separation between the antiferromagnetic Ru_2MnGe and the ferromagnetic Ru_2FeGe with long-range magnetic order in each phase. However, the XRD profile shows no peak separation.

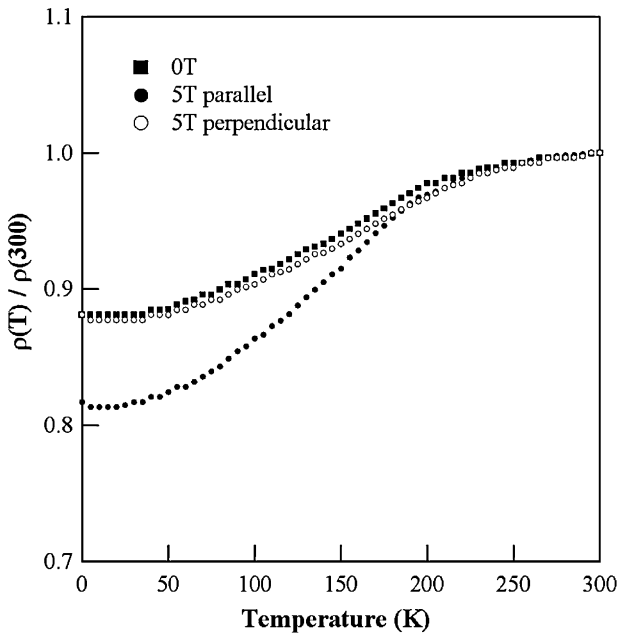

Fig. 6. Temperature dependence of the resistivity measured for $Ru_2Mn_{0.5}Fe_{0.5}Ge$ under applied field of 0 and 5 T perpendicular and parallel mean the geometry between electrical current and applied magnetic field.

In other cases, the mictomagnetism would be established in this region by the coexistence between the antiferromagnetic interaction based on Mn atoms, the ferromagnetic interaction based on Fe–Fe atoms, and the weak ferromagnetic interaction between Mn–Fe atom without long-range magnetic order. Ni_3Mn single crystal [22] shows the induction of the magnetic anisotropy by similar phenomenon. Then, the origin of this magnetism seems to be a mictomagnetism.

3.3. Transport properties

$Ru_2Mn_{1-x}Fe_xGe$ system shows metallic characteristic in the temperature dependence of the $\rho\,||\,(T)$ and $\rho\perp(T)$, where $\rho||$ and $\rho\perp$ are resistivity measured in the parallel and perpendicular configuration between electrical current and applied field, respectively. For $Ru_2Mn_{0.6}Fe_{0.4}Ge$, temperature dependence of $\rho||$ and $\rho\perp$ for under applied field of 0 T and 5 T shows an anisotropic MR effect in Fig. 6. $\rho||$ and $\rho\perp$ show a same temperature dependence under 0 T; however, although $\rho\perp$ under 5 T shows almost same temperature dependence with that of 0 T, $\rho||$ under 5 T shows a large negative MR effect at low temperature.

Fig. 7 shows temperature dependence of the MR ratio for $Ru_2Mn_{0.6}Fe_{0.4}Ge$ and $Ru_2Mn_{0.5}Fe_{0.5}Ge$. Both samples show relatively large anisotropic MR effect below T_C. In case of $Ru_2Mn_{0.6}Fe_{0.4}Ge$, as shown in Fig. 7(a), magnitude of the negative MR ratio of $\rho||$ increases monotonically as the temperature decreases; however, that of $\rho\perp$ is almost temperature independent. On the other hand, as shown in Fig. 7(b), magnitude of the negative MR ratio for $\rho||$ of $Ru_2Mn_{0.5}Fe_{0.5}Ge$ increases monotonically below 180 K, whereas that for $\rho\perp$ changes its sign from negative to positive at about 110 K. This result indicates that there is an anisotropic MR effect on the $Ru_2Mn_{1-x}Fe_xGe$ system, and that the MR effect occurs at low temperature, where the magnetic states are established.

Fig. 8 shows magnetic-field dependence of MR ratio for the sample of $x = 0.4$, 0.5 and 0.6 at 10 K. Although all samples show similar field dependence, the absolute value of saturated MR ratio changes with increasing Fe content. There are three noteworthy points for $Ru_2Mn_{0.5}Fe_{0.5}Ge$; (1) similar field dependence to that of the spin

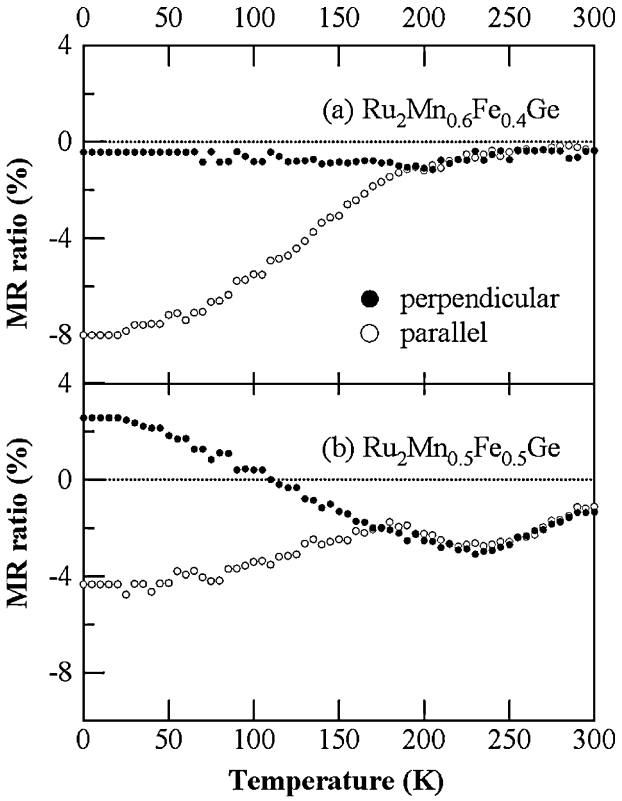

Fig. 7. (a) Temperature dependence of the magnetoresistance (MR) measured for specimen of $x = 0.4$ under applied field of 5 T and (b) that for $x = 0.5$. Perpendicular and parallel mean the geometry between current and applied magnetic field.

valve devices and (2) pronounced anisotropic MR effect, where negative or positive MR was observed depending on the geometry between applied field and electrical current. Similar MR effects to the present results are reported in the case of the $Co_2Cr_{0.6}Fe_{0.4}Al$

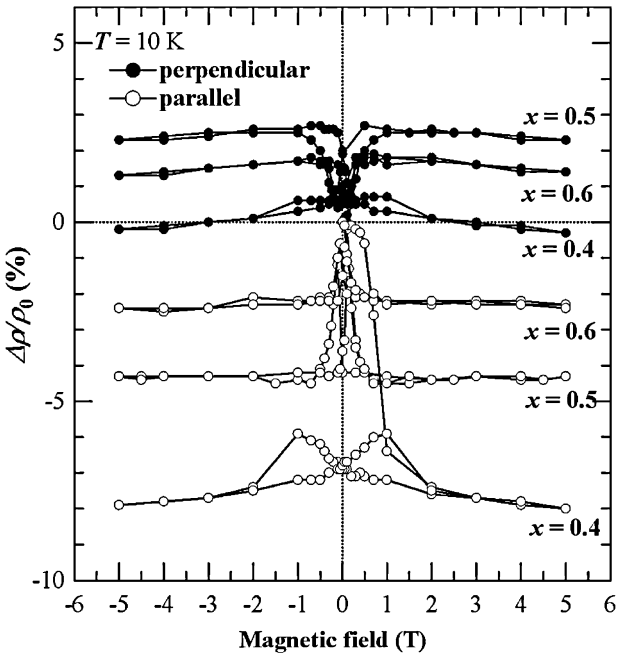

Fig. 8. Magnetic-field dependence of the magnetoresistance (MR) measured for specimen of $Ru_2Mn_{1-x}Fe_xG$ in the perpendicular (filled circle) and parallel (open circle) alignments at 10 K.

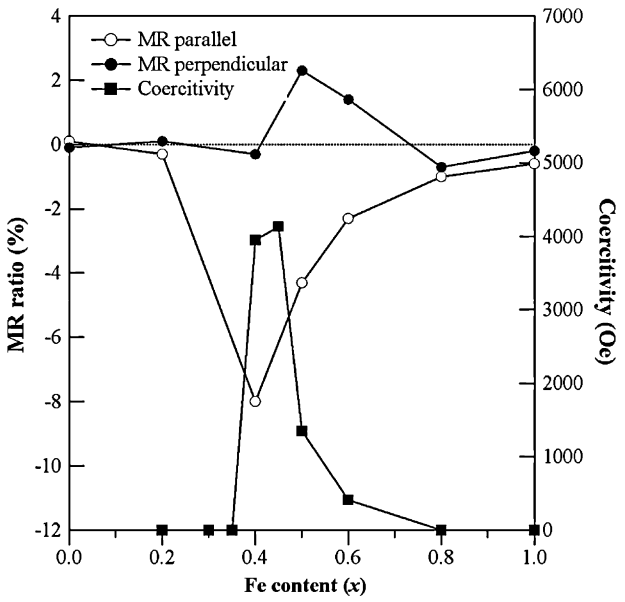

Fig. 9. Fe-content dependence of the MR ratio obtained for $Ru_2Mn_{1-x}Fe_xG$ in perpendicular (filled circle) and parallel (open circle) alignments at 10 K under an applied field of 5 T and the coercivity obtained at 5 K.

system. (3) The absolute MR effect ratio has a Fe content dependence.

Fig. 9 summarizes the MR ratio at 5 T and the coercivity at 10 K as a function of Fe content. These results suggest that the MR effect depend on the Fe content. MR ratio of the end-members, Ru_2MnGe and Ru_2FeGe, are negligibly small and large MR effect occurs only in the intermediate composition range in the $Ru_2Mn_{1-x}Fe_xGe$ system. The magnitude of the MR ratio for parallel and perpendicular configuration has a maximum at a composition of $Ru_2Mn_{0.6}Fe_{0.4}Ge$. This experimental result in Fig. 9 reveals a correlation between the variations of MR ratio with that of coercive field as a function of x. The composition range with the anisotropic MR effect is same as the appearance of large coercivity, where appears for samples of group-II ($0.4 \leq x \leq 0.6$). This similar trend suggests that the magnetic anisotropy is important for the present MR effect and implies that the induction of the MR effect and the coercivity is originated by the common mechanism.

From these results, we suggest the model of MR effect. The variation of the MR ratio and the coercivity in Fe content suggests that the large MR effect in the ferromagnetic group-II ($0.4 \leq x \leq 0.6$) induced by the mixed magnetic states to establish the strong competing magnetic states between the antiferromagnetic Mn–Mn exchange interaction, the antiferromagnetic Fe–Mn interaction, and the ferromagnetic Fe–Fe interaction. This competing magnetic state stabilizes the quasi-stable ferromagnetic state. Therefore, the suppression of the spin scattering between the spin moment and the conduction electrons would induce the decrease of the resistivity below T_C under external magnetic fields. Moreover, the appearance of anisotropic MR effect would be caused by the same reason of the hysteresis loop which induced by the coexistence and the competition between the antiferromagnetic interaction and the ferromagnetic interaction. The correlation between the appearance of the hysteresis loop and the MR effect would be as follows. Antiferromagnetic Mn moments are aligned along the [1 1 1] direction, and the antiferromagnetic Mn moment will pin nearest neighbor ferromagnetic Fe moment via exchange interaction. The pinning of the ferromagnetic Fe moment induce the anisotropic spin scattering between the ferromagnetic moment and the conduction electrons since the direction of Fe moment align to the competing direction between the direction

along the external magnetic fields and along the direction of Mn moment. This seems to be an origin of MR observed for $Ru_2Mn_{1-x}Fe_xGe$ system at intermediate compositions. The mixed magnetic states model can explain the relatively large MR effect for $Ru_2Mn_{1-x}Fe_xGe$ system. Moreover, the present observations are evidence for the macroscopic separation and for the strongly relation between the macroscopic separation and the induction of the anomalous physical properties. Therefore, the MR effect in this system seems to differ from that of $Co_2Cr_{0.6}Fe_{0.4}Al$ [6] in the mechanism with the half metallic electronic structure.

4. Conclusion

The structural, the magnetic, and the transport properties were studied for bulk polycrystalline Heusler alloys with composition of $Ru_2Mn_{1-x}Fe_xGe$ to reveal the correlation between the magnetic properties and the composition x. The experimental results show a similar trend and a correlation between the variations in MR ratio with that of coercive field as a function of x. The appearance of the ferromagnetic with anisotropic MR effect is shown at the boundary of magnetism between antiferromagnetic and soft ferromagnetic. This implies that the MR effect in this system needs proper mixed magnetic exchange interaction to establish the strong competing magnetic states between the antiferromagnetic interaction and the ferromagnetic interaction, which would be caused by the macroscopic phase separation.

Acknowledgments

The work done at Aoyama Gakuin University was supported by The Private School High-tech Research Center Program of the MEXT, Japan. A part of this work was supported by the Sasakawa Scientific Research Grant from The Japan Science Society.

References

[1] R.A. de Groot, F.M. Mueller, P.G. Engen, K.H. Buschow, Phys. Rev. Lett. 50 (1983) 2024.
[2] J. Kubler, A.R. Williams, C.B. Sommers, Phys. Rev. B 28 (1983) 1745.
[3] P.J. Brown, K.U. Neumann, P.J. Webster, K.R.A. Ziebeck, J. Phys.: Condens. Matter 12 (2000) 1827.
[4] K. Inomata, S. Okamura, R. Goto, N. Tezuka, Jpn. J. Appl. Phys. 42 (2003) L419.
[5] T. Marukame, T. Ishikawa, S. Hakamata, K. Matsuda, T. Uemura, M. Yamamoto, Appl. Phys. Lett. 90 (2007) 012508.
[6] T. Block, C. Felser, G. Jakob, J. Ensling, B. Mühling, P. Gütlich, R.J. Cava, J. Solid State Chem. 176 (2003) 646.
[7] C. Felser, B. Heitkamp, F. Kronast, D. Schmitz, S. Cramm, H.A. Dürr, H.-J. Elmers, G.H. Fecher, S. Wurmehl, T. Block, D. Valdaitsev, S.A. Nepijko, A. Gloskovskii, G. Jakob, G. Schönhense, W. Eberhardt, J. Phys.: Condens. Matter 15 (2003) 7019.
[8] M. Buchmeier, C.M. Schneider, J. Werner, D. Elefant, A. Teresiak, G. Behr, J. Schumann, E. Arushanov, J. Magn. Magn. Mater. 313 (2007) 157.
[9] D. Serrate, J.M. De Teresa, R. Cordoba, S.M. Yusuf, Solid State Commun. 142 (2007) 363.
[10] V.N. Antonov, H.A. Durr, Yu. Kucherenko, L.V. Bekenov, A.N. Yaresko, Phys. Rev. B 72 (2005) 054441.
[11] Y. Miura, M. Shirai, K. Nagao, J. Appl. Phys. 95 (2004) 7225.
[12] Y. Miura, K. Nagao, M. Shirai, Phys. Rev. B 69 (2004) 144413.
[13] I. Galanakis, P.H. Dederichs, N. Papanikolaou, Phys. Rev. B 66 (2002) 174429.
[14] V.S. Patil, R.G. Pillay, P.N. Tandon, H.G. Devare, Phys. Stat. Sol. (b) 118 (1983) 57.
[15] A. Szytula, H. Ptasiewicz-Bak, J. Leciejewicz, J. Magn. Magn. Mater. 80 (2–3) (1989) 195.
[16] T. Kanomata, M. Kikuchi, H. Yamauchi, J. Alloys Compd. 414 (1–2) (2006) 1.
[17] S. Ishida, S. Kashiwagi, S. Fujii, S. Asano, Physica B 210 (1995) 140.
[18] T. Graf, J. Barth, C.G.F. Blum, B. Balke, C. Felser, Phys. Rev. B 82 (2010) 104420.
[19] M. Gotoh, M. Ohashi, T. Kanomata, Y. Yamaguchi, Physica B 306 (1995), 213, 214.
[20] J. Kubler, G.H. Fecher, C. Felser, Phys. Rev. B 76 (2007) 024414.
[21] S. Chikazumi, C.D. Graham Jr., Physics of Ferromagnetism, Clarendon, Oxford, 1997.
[22] T. Satoh, J. Phys. Soc. Jpn. 21 (1966) 1892.